Journal of Alloys and Compounds 520 (2012) 132–139

Contents lists available at SciVerse ScienceDirect

Journal of Alloys and Compounds

journal homepage: www.elsevier.com/locate/jallcom

Investigation of the microstructure, magnetic and microwave properties of electrodeposited Ni_xFe_{1-x}(x = 0.2–0.76) films

L.X. Phua[a,*], N.N. Phuoc[b], C.K. Ong[a]

[a] Centre for Superconducting and Magnetic Materials, Department of Physics, National University of Singapore, 2 Science Drive 3, Singapore 117542, Singapore
[b] Temasek Laboratories, National University of Singapore, 5A Engineering Drive 2, Singapore 117411, Singapore

ARTICLE INFO

Article history:
Received 21 September 2011
Received in revised form
28 December 2011
Accepted 29 December 2011
Available online 14 January 2012

Keywords:
Thin films
Magnetic measurements

ABSTRACT

The microstructure, magnetic properties and microwave characteristics of NiFe films were investigated with chemical composition variation. It was found that Ni concentration has a strong influence on film stress and film surface roughness which induces variations in static and dynamic anisotropy field. Also, with the variation of Ni concentration, there is a spin-reorientation behavior which may be attributed to the contribution of the magnetic anisotropy originating from the composition gradient and the anisotropy induced by deposition field. Ferromagnetic resonance and rotatable magnetic anisotropy were observed for Ni_xFe_{1-x} (x = 0.51–0.76) films. The results were discussed based on Landau–Lifshitz–Gilbert equation and magnetic ripple theory. The rotatable anisotropy field was highly correlated to the film surface roughness. The ferromagnetic resonance varied from 0.589 to 0.886 GHz as Ni concentration was increased from 0.51 to 0.76 wt. ratio.

1. Introduction

Magnetic thin films have been widely utilized in many electronic devices. Alloys of Ni_xFe_{1-x} are known to possess excellent soft magnetic properties such as high permeability, low coercivity and high stability against corrosion. Hence they are used in a variety of industrial application such as inductor cores for electromagnet [1], magnetic recording head [2–4], magnetic devices [5], inductor cores [6,7], microwave noise filters [8] and tunable noise suppressor [9]. Ni_xFe_{1-x} thin films were most commonly fabricated by sputtering [10–12] and electrodeposition [2,7] methods. Compared to conventional sputtering technique, electrodeposition method has several advantages such as low cost and the possibility of mass production, which are suitable for industrial application. This method also allows fine tuning of magnetic properties of fabricated thin films by varying the deposition conditions and is able to provide uniform, low temperature and large area formation of soft magnetic thin film on complex geometry. Low temperature fabrication enables soft magnetic thin films to be deposited directly onto many magnetic and electronic devices without any heat treatment that may damage the devices, and hence, this will further widen the application range of soft magnetic thin films. Among many studies on magnetic thin films fabricated by electrodeposition method, however, there have been few works focusing on the microwave properties of those films. Taking into consideration the fact that magnetic thin films have found many applications in electronic devices operating in high frequency, a systematic study of dynamic properties of magnetic thin films may be useful for researchers in the field. Hence, in this study, we report about our investigation of the dynamic and static magnetic properties of Ni_xFe_{1-x} (x = 0.2–0.76) films fabricated by electrodeposition technique at room temperature. We will conduct a comprehensive study of magnetic thin film properties over a wide range of chemical composition variation.

2. Experimental procedures

Electrodeposition was preformed in an electrochemical cell using a current generator (Advantest R6142) with two facing vertical electrodes flushed to the side walls to achieve a uniform current distribution. The anode was a copper-taped carbon rod (Morganite Carbon) and the cathode was the depositing substrate. The substrates used in this study were silica glass substrates sputtered with Ti (50 nm) and Cu (100 nm) seed layers, with Cu layers being on the top to act as an anode for electrodeposition. A magnetic field of 100 Oe was applied along the plane of substrate during film growth to achieve uniaxial in-plane anisotropy. In this work, Ni(0.20–0.76 wt. ratio)Fe(0.80–0.24 wt. ratio) soft magnetic films were fabricated. The deposition bath composition and deposition condition are reported in Table 1.

A Vibrating-Sample Magnetometer (VSM, DMS-VSM 886) was employed to characterize the static magnetic properties of the films. The morphology of

* Corresponding author at: Centre for Superconducting and Magnetic Materials, Department of Physics, National University of Singapore, 2 Science Drive 3, Singapore 117542, Singapore. Tel.: +65 65166238.
E-mail address: g0700691@nus.edu.sg (L.X. Phua).

0925-8388/$ – see front matter © 2012 Elsevier B.V. All rights reserved.
doi:10.1016/j.jallcom.2011.12.164

Table 1
Bath composition and deposition condition.

Electrodeposition bath composition	
$NiSO_4{\cdot}6H_2O$	0.2 M
$FeSO_4{\cdot}7H_2O$	0.06–0.1 M
NH_4Cl	0.28 M
H_3BO_3	0.4 M
Sodium dodecyl sulfate	0.01 g/L
Deposition condition	
Current density	3 mA cm^{-2}
Deposition time	5 min
Deposition temperature	25 °C

fabricated film was analyzed with Field Emission Scanning Electron Microscope (SEM, Joel JSM 6701F). The domain structure of Ni_xFe_{1-x} (x = 0.2–0.76) films was analyzed by Magnetic Force Microscope (MFM, DI 3000). The crystallographic film structure was characterized by an X-ray diffractometer with Cu-$K\alpha$ radiation (XRD, Philips Analytical X-Ray Diffractometer, PW1820/00). Permeability measurement of film was performed with shorted microstrip transmission-line perturbation method previously developed in our laboratory [13].

3. Results and discussion

Fig. 1 shows the XRD scans of Ni_xFe_{1-x} (x = 0.65–0.76) electrodeposited films with various compositions. The result shows that both $Ni_{0.65}Fe_{0.35}$ (Fig. 1-(a)) and $Ni_{0.68}Fe_{0.32}$ (Fig. 1-(b)) films have a mixture of both fcc and bcc structure [3]. As Fe content is decreased in $Ni_{0.72}Fe_{0.28}$ and $Ni_{0.76}Fe_{0.24}$ films, bcc phase is subdued and deposited films consist of only fcc phase. For Ni_xFe_{1-x} (x = 0.2–0.51) films with low concentration of Ni, the XRD profiles show a similar trend as in the $Ni_{0.65}Fe_{0.35}$ film (Fig. 1-(a)).

The SEM images in Fig. 2 show that all films have grain-like structure. $Ni_{0.2}Fe_{0.8}$ and $Ni_{0.65}Fe_{0.35}$ films have elongated grains while all other films have rounded grains. Fig. 2(c) and (d) shows that in both $Ni_{0.4}Fe_{0.6}$ and $Ni_{0.51}Fe_{0.49}$ films, small grains have coalesced to form a smoother film cross section. In Fig. 2-(e), the grains in $Ni_{0.65}Fe_{0.35}$ film show the tendency of growing into column-like morphology. All films show good adhesion with silica glass substrate. The thickness of film varies from 0.580 to 1.260 μm.

Thin films of Ni_xFe_{1-x} (x = 0.20–0.51) show distinct grains on the film surface in Fig. 3(a)–(d). As Ni concentration is increased and at the same time Fe concentration is decreased, the grain size is decreased and the film surface become smoother as shown in Fig. 3(e)–(h). Hence an increase in Fe concentration result in increased grain growth and conversely, an increase in Ni content inhibit grain growth and result in smaller grain size and smoother film surface. Similar grain growth and film surface roughness observation with Ni concentration variation was reported by Zhang et al. [14].

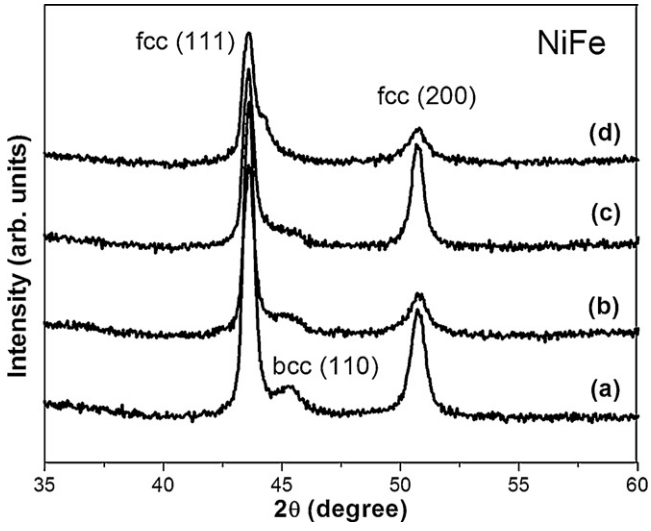

Fig. 1. XRD scan of (a) $Ni_{0.65}Fe_{0.35}$, (b) $Ni_{0.68}Fe_{0.32}$, (c) $Ni_{0.72}Fe_{0.28}$ and (d) $Ni_{0.76}Fe_{0.24}$ films.

The hysteresis loops of Ni_xFe_{1-x} (x = 0.2–0.76) films with various compositions measured along the in-plane parallel and in-plane perpendicular directions are presented in Fig. 4. The in-plane parallel direction is defined as the direction of the magnetic field applied during electrodeposition while the in-plane perpendicular is the direction normal to the deposition magnetic field but still in the plane of films. For the sake of simplicity, hereafter, the magnetization curves measured along in-plane parallel and in-plane perpendicular directions will be denoted as parallel curve and perpendicular curve, respectively. It is of great interest to observe a spin-reorientation behavior with the change of composition. In particular, when the Ni composition is varied from 0.2 to 0.4, the easy axis tends to orient along in-plane perpendicular direction as seen in the magnetization curves shown in Fig. 4-(a)–(c), although the distinction between the parallel curve and perpendicular curve in Fig. 4-(a) and (b) is not clear. However, the perpendicular curve in Fig. 4-(c) clearly demonstrates that it behaves like an easy axis that unambiguously indicates that a magnetic anisotropy is present in this sample with the easy axis along the perpendicular direction. As the Ni composition is further increased from 0.51 to 0.76, the parallel and perpendicular curves first looked almost identical and then gradually become different again but with the easy axis is now oriented along the parallel direction. In other words, for Ni_xFe_{1-x} films with x = 0.2–0.4 the magnetic anisotropy tends to orient along the direction perpendicular to the magnetic field applied during deposition while it is oriented along the deposition field direction with x = 0.51–0.76. For the latter case, the behavior is quite usual as often observed in the films deposited by other methods such as sputtering [15], namely the magnetic anisotropy present in the films is due to the induced anisotropy created by the magnetic field during deposition. For the former case, i.e. the magnetic anisotropy easy axis is perpendicular to the deposition field, the reason may tentatively be due to the influence of the composition gradient present in the films. It is well-known in the literature that the magnetic force applied during electrodeposition has a strong influence on the mass transport [16]. This may cause an inhomogeneous composition in the NiFe films. In particular, the composition of NiFe along the deposition magnetic field may be varied and this variation consequently produces some gradient of the composition along the direction normal to deposition field but still in the film's plane. This composition gradient results in a magnetic anisotropy parallel with the composition gradient normal to the deposition field. It is noticed that the magnetic anisotropy induced by the composition gradient is present in all the NiFe samples and this anisotropy may compete with the magnetic anisotropy induced by the deposition field. Hence it may show its dominance over the other anisotropy in some composition and is dominated by the other anisotropy in some other composition. That explains why there is a spin-reorientation behavior. Previously, there were several observations on the magnetic anisotropy induced by the composition gradient in the magnetic thin films fabricated by sputtering technique with special set up [17,18]. Our interpretation of this behavior in terms of the gradient composition influence is thus quite reasonable. However, further experiments are needed to verify this argument.

The Magnetic Force Microscope (MFM) image in Fig. 5 shows that distinct strip domains exist within $Ni_{0.4}Fe_{0.6}$ film. All other Ni_xFe_{1-x} (x = 0.2–0.76) films show similar MFM images as in Fig. 5. Previous studies by Dastagir et al. [6] and Zou et al. [19] proves that strip domains exist in NiFe films. This result is in reasonable agreement with the hysteresis loops, in the sense that the hysteresis

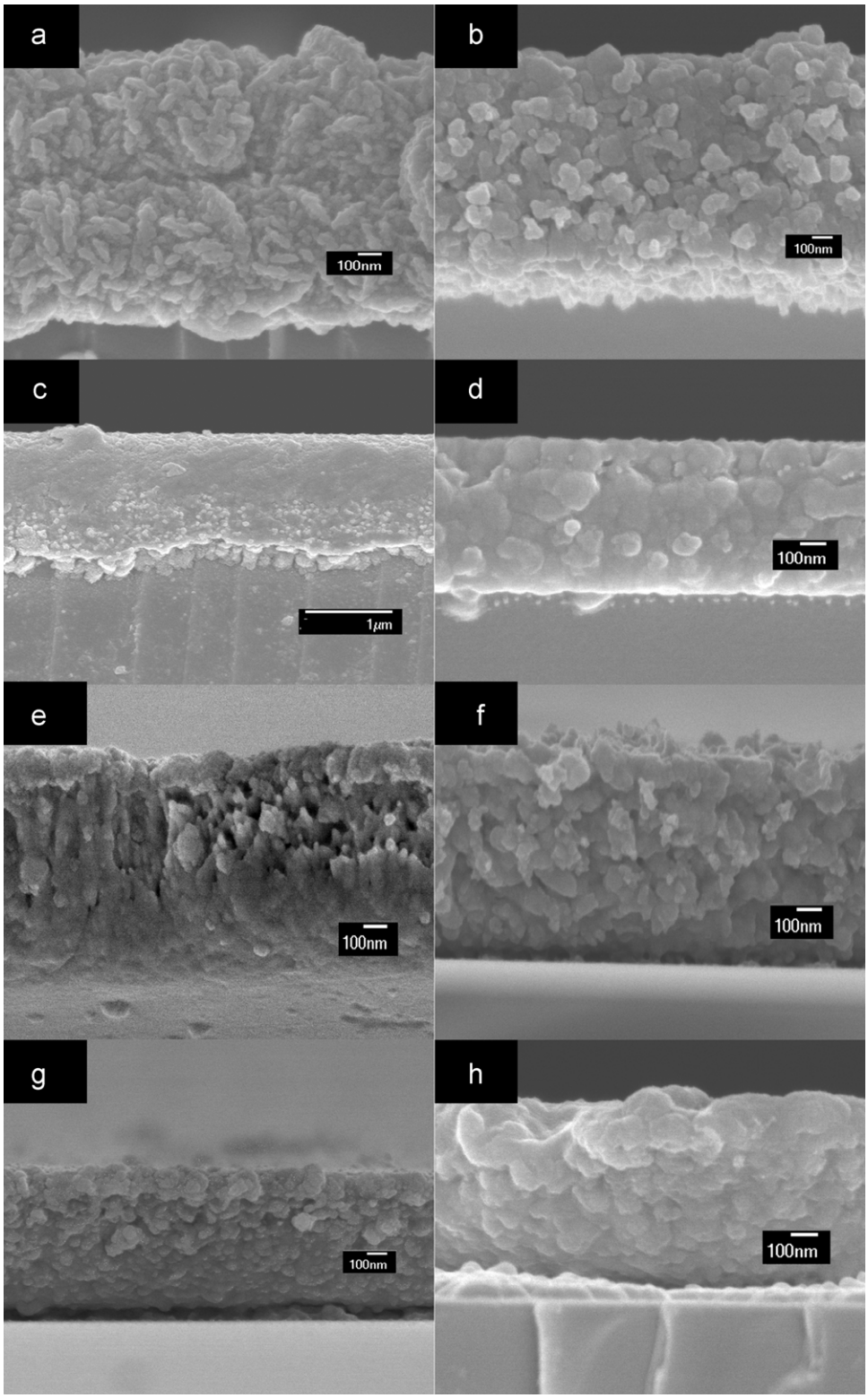

Fig. 2. SEM cross-section morphology of Ni_xFe_{1-x} films with various compositions: (a) $x = 0.20$, (b) $x = 0.30$, (c) $x = 0.40$, (d) $x = 0.51$, (e) $x = 0.65$, (f) $x = 0.68$, (g) $x = 0.72$ and (h) $x = 0.76$.

loops show a typical characteristic curve near to saturation magnetization which is similar to the observations by Dastagir et al. [6] and Zou et al. [19].

Presented in Fig. 6-(a) are the coercivities derived from the hysteresis loops measured along parallel and perpendicular directions as a function of Ni concentration. All the samples show low coercivity less than 10 Oe, except for the case of Ni concentration $x = 0.4$. This high value of coercivity may presumably be owing to the high magnetic anisotropy originating from composition gradient as discussed above. As shown in Fig. 6-(b),

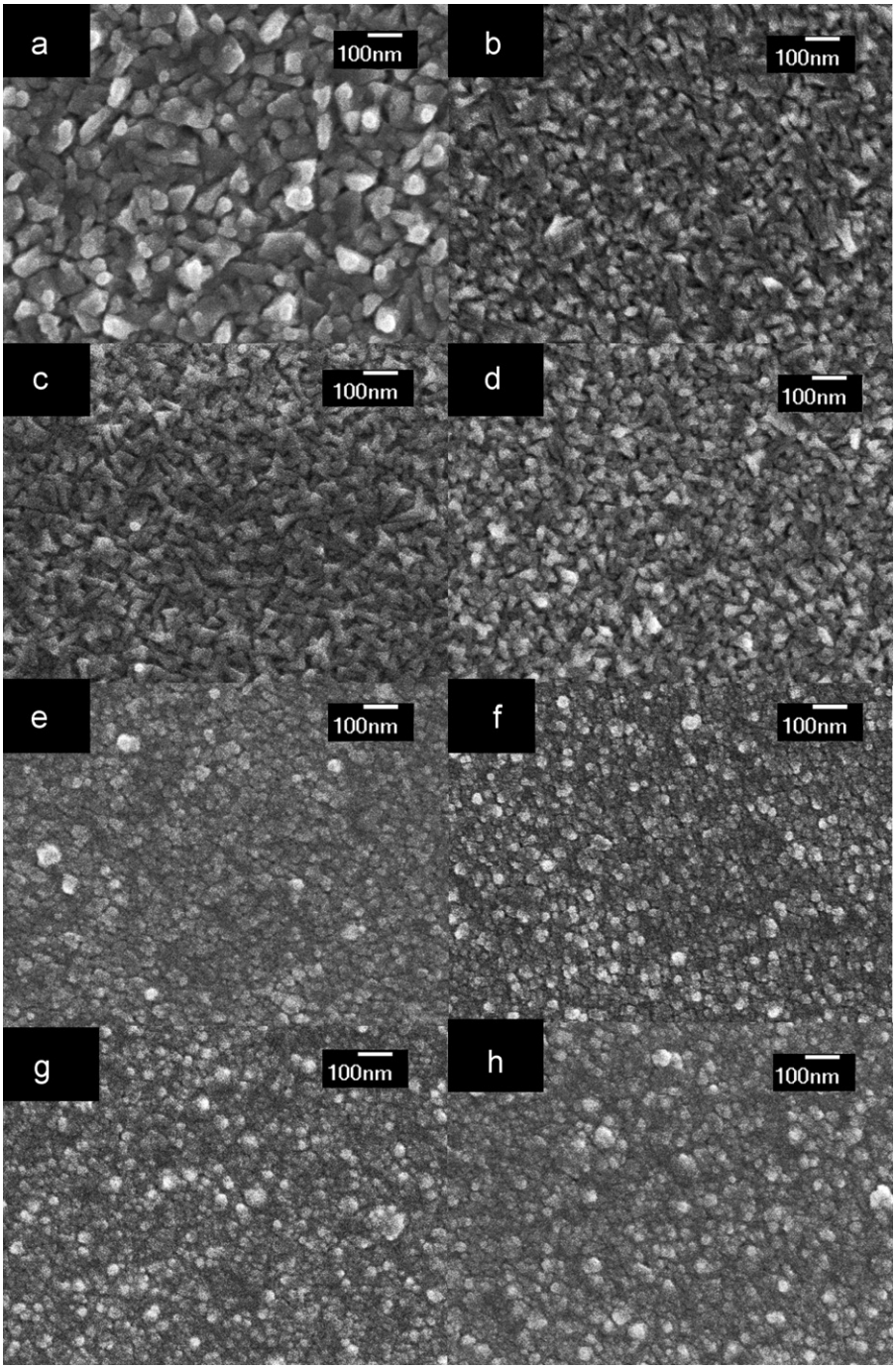

Fig. 3. SEM top-view pictures showing the morphologies of Ni_xFe_{1-x} films with various compositions: (a) $x = 0.20$, (b) $x = 0.30$, (c) $x = 0.40$, (d) $x = 0.51$, (e) $x = 0.65$, (f) $x = 0.68$, (g) $x = 0.72$ and (h) $x = 0.76$.

in-plane parallel saturation magnetization has the highest value of 515 emu/cc at $Ni_{0.51}Fe_{0.49}$ film. The present coercivity and saturation magnetization values are comparable to the values of NiFe films fabricated by sputtering technique reported in the literature [12].

Fig. 7 shows the permeability spectrum of Ni_xFe_{1-x} ($x = 0.51$–0.76) films. Ni_xFe_{1-x} ($x = 0.2$–0.4) films show no ferromagnetic resonance (FMR). The FMR peak shifts from 0.589 GHz to 0.886 GHz as Ni concentration is increased. A quantitative examination of the effect of film properties on the dynamic properties of film is conducted by an analysis based on the Landau–Lifshitz–Gilbert (LLG) fitting. The dynamic magnetization behavior of thin film was described by the LLG equation [20],

$$\frac{d\vec{M}}{dt} = -\gamma(\vec{M} \times \vec{H}) + \frac{\alpha_{eff}}{M}\vec{M} \times \frac{d\vec{M}}{dt} \quad (1)$$

where M represents the magnetic moment, H is the magnetic field, α_{eff} is the dimensionless effective damping coefficient and γ is the gyromagnetic ratio.

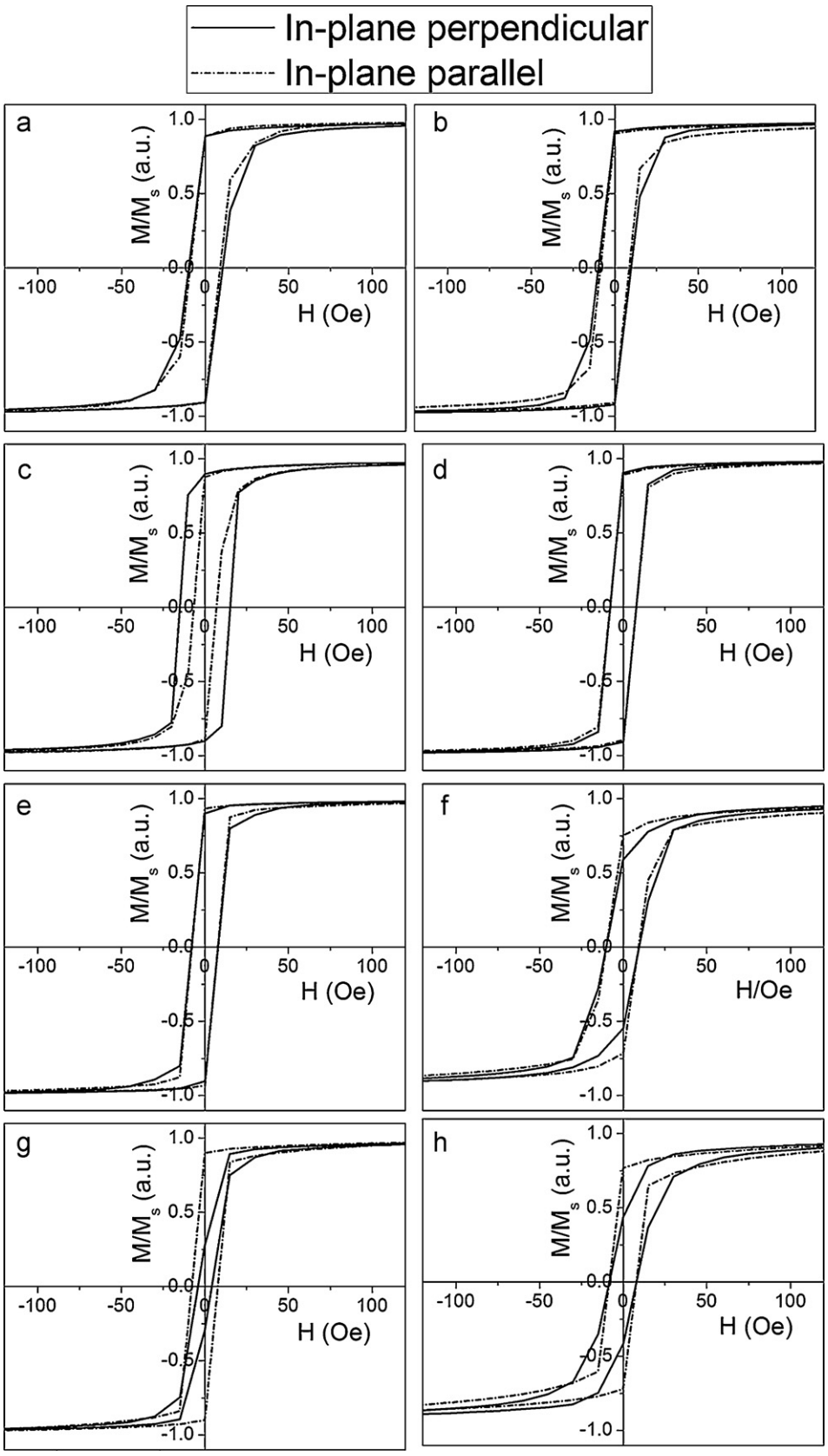

Fig. 4. Hysteresis loop of Ni_xFe_{1-x} films where x = (a) 0.20, (b) 0.30, (c) 0.40, (d) 0.51, (e) 0.65, (f) 0.68, (g) 0.72 and (h) 0.76.

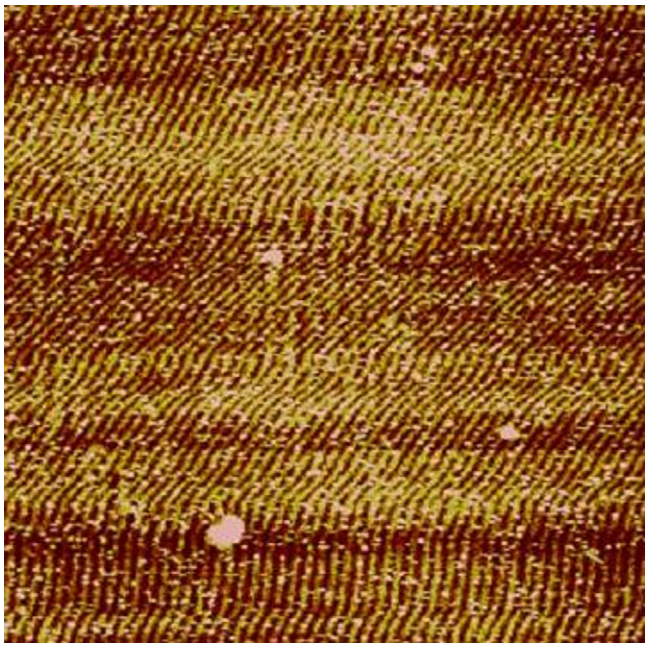

Fig. 5. 30 μm × 30 μm MFM image of $Ni_{0.4}Fe_{0.6}$ film. (Color image is available online).

Solving the LLG equation, one can obtain the complex permeability as follows [21–23]:

$$\mu' = 1 + 4\pi M_{eff}\gamma^2 \frac{(4\pi M_{eff} + H_K^{dyn})(1+\alpha_{eff}^2)[\omega_R^2(1+\alpha_{eff}^2) - \omega^2] + (4\pi M_{eff} + 2H_K^{dyn})(\alpha_{eff}\omega)^2}{[\omega_R^2(1+\alpha_{eff}^2) - \omega^2]^2 + [\alpha_{eff}\omega\gamma(4\pi M_{eff} + 2H_K^{dyn})]^2} \quad (2)$$

$$\mu'' = 4\pi M_{eff}\gamma\omega\alpha_{eff} \frac{(4\pi M_{eff} + H_K^{dyn})^2(1+\alpha_{eff}^2) + \omega^2}{[\omega_R^2(1+\alpha_{eff}^2) - \omega^2]^2 + [\alpha_{eff}\omega\gamma(4\pi M_{eff} + 2H_K^{dyn})]^2} \quad (3)$$

where M_{eff}, H_K^{dyn} and ω_R ($\omega_R = 2\pi f_{FMR}$) are the effective magnetization, dynamic magnetic anisotropy and FMR angular frequency, respectively. Taking M_{eff}, H_K^{dyn} and α_{eff} as fitting parameters, Eqs. (2) and (3) can be used to fit the experimental curves in Fig. 7 quite well.

A decrease of Fe content results in a reduction of stress in NiFe films. This decrease was observed by Koo and Yoo [2] when they studied the relation between variation of Fe concentration and the resulting effect on film stress. This implies that the decrease of film stress has resulted in the shift of FMR peak to higher frequency range.

The dependence of H_K^{dyn} on Ni concentration is plotted in Fig. 8-(a). H_K^{sta} obtained from the slope of in-plane perpendicular hysteresis loop represents rotational like magnetization [24] and is also plotted in Fig. 8-(a) for comparison. There is a disparity between H_K^{dyn} and H_K^{sta} as shown in Fig. 8-(a), which has been observed in various soft magnetic thin films [25] and can be explained by Hoffmann's ripple theory [26]. According to this theory, there is an additional effective isotropic field that contributes to the anisotropy field obtained from permeability spectra beside the static intrinsic anisotropy field. This additional effective field depends on a ripple constant that originate from the local anisotropies which are in isotropic distribution [27,28] and consequently, it is not included in H_K^{sta} from the static measurement and hence contributes to the difference from the dynamic measurement [29]. $H_{rot}\left(=\left|H_K^{sta} - H_K^{dyn}\right|\right)$ is defined as the rotatable magnetic anisotropy field (the dynamically induced magnetic ripple field [29,30]). The variation of H_{rot} with Ni concentration is presented in Fig. 8-(b), showing a complicated behavior of H_{rot} as a function of Ni concentration. Previous studies claimed that the magnetic ripple field is induced by increased film surface roughness [29] and as a result, one may expect that there is an increase of H_{rot} with the surface roughness. However, in our films such a correlation is not clearly evident.

From the experimental permeability plot in Fig. 7, one can estimate the FMR frequency (f_{FMR}) by determining the peak position but this is not easy for the case of broad frequency linewidth. Hence, it is more accurate to derive f_{FMR} from the LLG fitting curves in Fig. 7. In particular, one can obtain f_{FMR} by using the Kittel equation [31], which reads,

$$f_{FMR} = \frac{\gamma}{2\pi}\sqrt{H_K^{dyn}(H_K^{dyn} + 4\pi M_{eff})} \quad (4)$$

The dependence of f_{FMR}, α_{eff} and frequency linewidth (Δf) on Ni wt. ratio are shown in Fig. 9-(a). α_{eff} is obtained from LLG

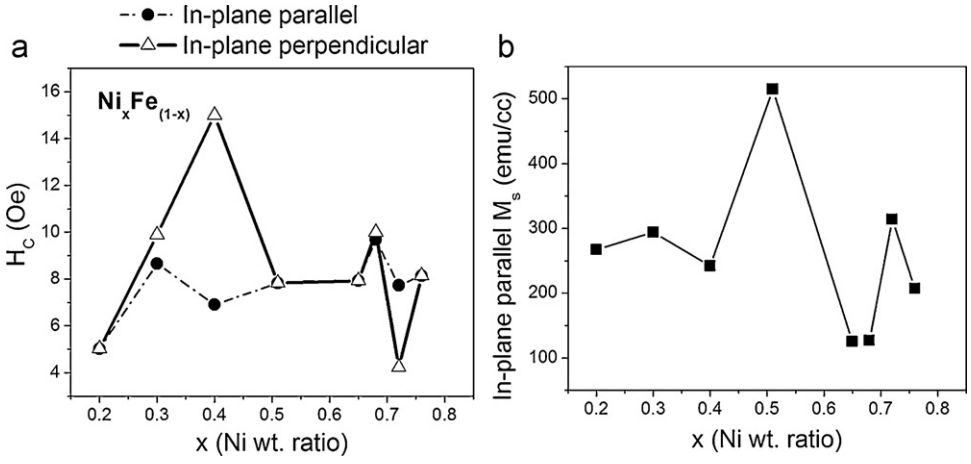

Fig. 6. (a) In-plane parallel and perpendicular hysteresis loop coercivities and (b) in-plane parallel saturation magnetization of Ni_xFe_{1-x} films.

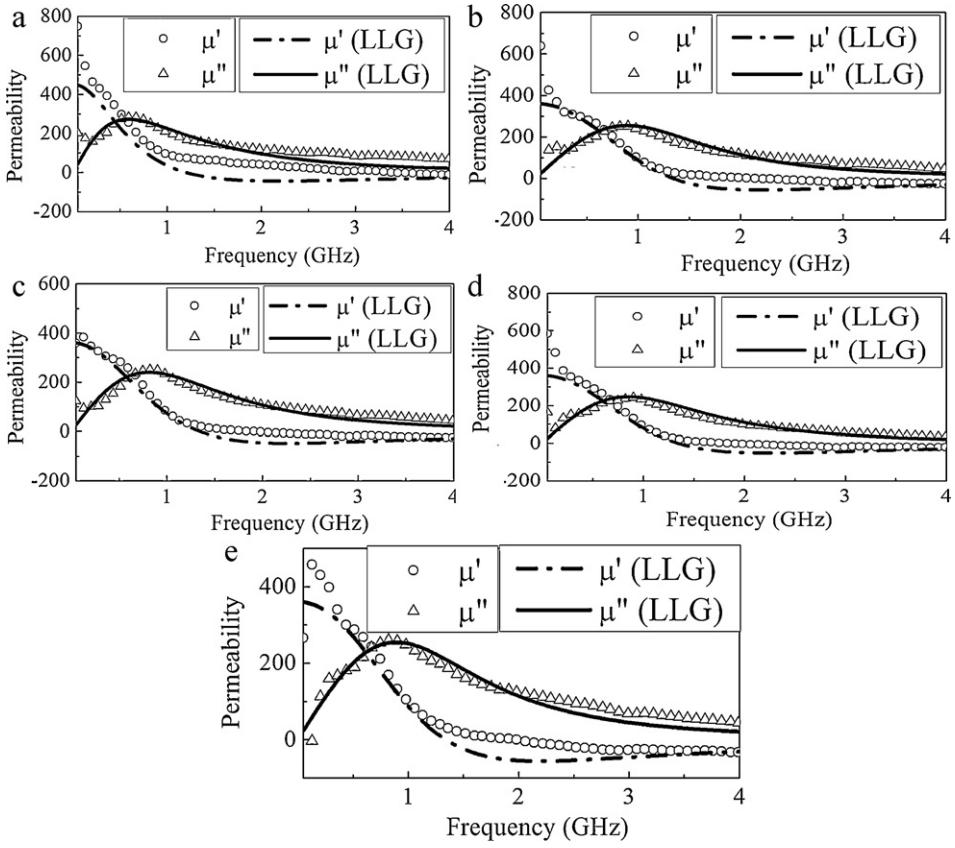

Fig. 7. Permeability spectrum of Ni_xFe_{1-x} films with x = (a) 0.51, (b) 0.65, (c) 0.68, (d) 0.72 and (e) 0.76.

curve-fitting and Δf is determined from the following formula [32]:

$$\Delta f = \frac{\gamma \alpha_{eff}(4\pi M_{eff} + 2H_K^{dyn})}{2\pi} \quad (5)$$

f_{FMR} is increased as Ni concentration is increased as shown in Fig. 9-(a). A similar observation was seen in Fig. 7. Hence, experimental FMR frequency variation agrees well with the theoretical prediction given in Eq. (4). From Eq. (4), f_{FMR} varies linearly with H_K^{dyn}. Hence, the increase in H_K^{dyn} with Ni addition in Fig. 8-(a) results in the corresponding variation in FMR frequency with Ni concentration. In Fig. 9-(a), Δf varies linearly with α_{eff} since H_K^{dyn} variation is small and $4\pi M_{eff}$ is a constant value for x = 0.51–0.76. Frequency linewidth is reduced as Ni concentration is increased. This reduction is possibly caused by a reduction of film stress with Ni addition which results in dispersion of the magnetic anisotropy of thin films due to the stress effect in ripple theory.

Fig. 9-(b) shows the variations of static permeability (μ_S) which is derived from the LLG curves at zero frequency. μ_S is known to depend on the effective magnetization (M_{eff}) and static magnetic anisotropy field H_K^{sta} as below [33]:

$$\mu_S = 1 + \frac{M_{eff}}{H_K^{sta}} \quad (6)$$

As given by Eq. (6), the increase in H_K^{sta} with Ni increment in Fig. 8-(a) results in a corresponding decrease in μ_S with increased Ni concentration.

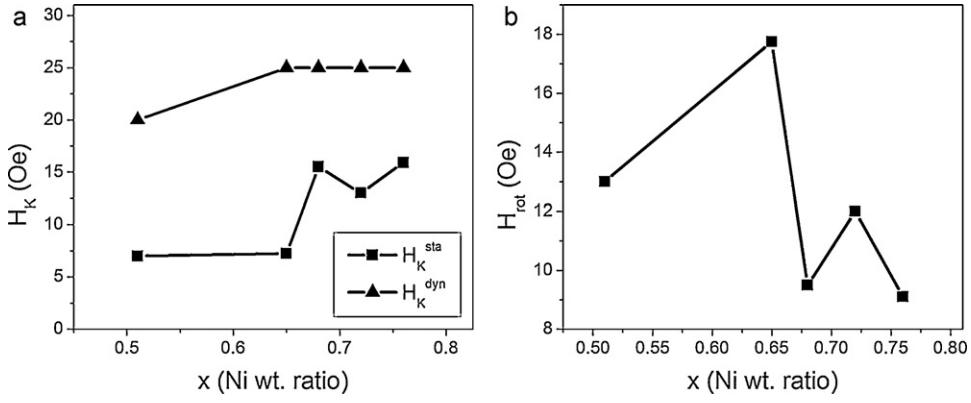

Fig. 8. (a) Static (H_K^{sta}) and dynamic (H_K^{dyn}) magnetic anisotropy field dependence and (b) rotatable anisotropy field dependence on Ni concentration.

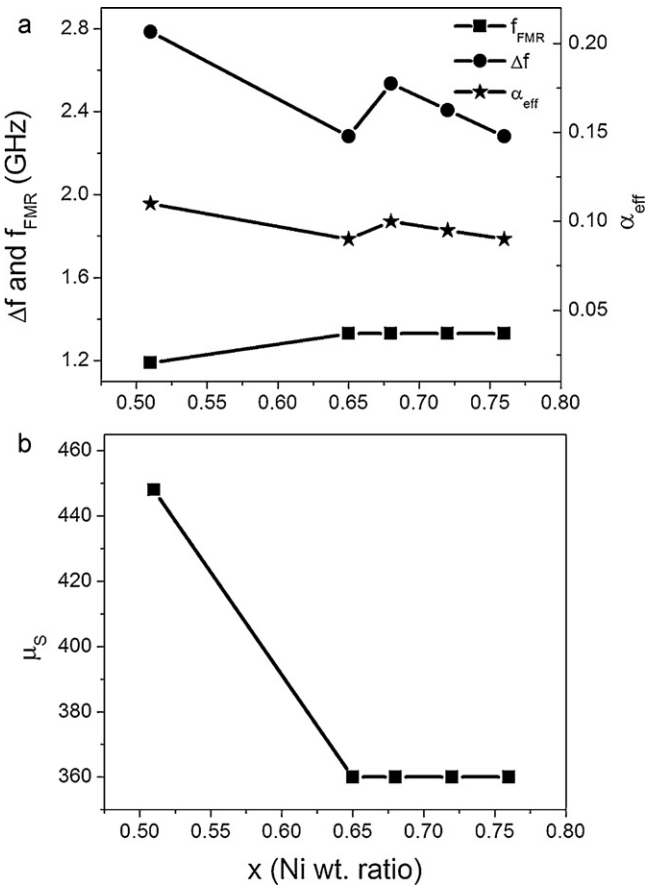

Fig. 9. (a) FMR frequency (f_{FMR}), frequency linewidth (Δf) and effective damping coefficient (α_{eff}) variation and (b) static permeability (μ_S) variation with Ni concentration.

4. Conclusion

In this paper, we investigate the effect of chemical composition variation on the magnetic properties and microwave characteristics of electrodeposited Ni_xFe_{1-x} films. It was found that with the increase of Ni concentration, the film surface roughness has reduced. In the low Ni concentration ($x = 0.2–0.4$), the easy axis is normal to the deposition field while in the high Ni concentration ($x = 0.51–0.76$) the easy axis is along the deposition field. This reorientation of easy axis is interpreted in terms of the competition between the magnetic anisotropy originating from composition gradient and the magnetic anisotropy induced by deposition field. We found the existence of ferromagnetic resonance and rotatable magnetic anisotropy in Ni_xFe_{1-x} ($x = 0.51–0.76$) films. The ferromagnetic resonance frequency is increased with Ni addition due to enhanced dynamic anisotropy field and the frequency linewidth is decreased with Ni addition due to reduced film stress.

Acknowledgment

The financial support from the Defence Research and Technology Office (DRTech) of Singapore for this work is gratefully acknowledged.

References

[1] E. Kubo, N. Ooi, H. Aoki, D. Watanabe, J.H. Jeong, C. Kimura, T. Sugino, Jpn. J. Appl. Phy. 49 (2010) 04DB17.
[2] B. Koo, B. Yoo, Surf. Coat. Technol. 205 (2010) 740.
[3] E.I. Cooper, C. Bonhote, J. Heidmann, Y. Hsu, P. Kern, J.W. Lam, M. Ramasubramanian, N. Robertson, L.T. Romankiw, IBM J. Res. Dev. 49 (2005) 103.
[4] T. Osaka, T. Asahi, J. Kawaji, T. Yokoshima, Electrochim. Acta 50 (2005) 4576.
[5] O. Song, C.A. Ballentine, R.C. O'Handley, Appl. Phys. Lett. 64 (1994) 2593.
[6] T. Dastagir, W. Xu, S. Sinha, H. Wu, Y. Cao, H. Yu, Appl. Phys. Lett. 97 (2010) 162506.
[7] T. O'Donnell, N. Wang, S. Kulkarni, R. Meere, F.M.F. Rhen, S. Roy, S.C. O'Mathuna, J. Magn. Magn. Mater. 322 (2010) 1690.
[8] C. Jiang, D. Xue, W. Sui, Thin Solid Films 519 (2011) 2527.
[9] B.K. Kuanr, R. Marson, S.R. Mishra, A.V. Kuanr, R.E. Camley, Z.J. Celinski, J. Appl. Phys. 105 (2009) 07A520.
[10] J. Vernieres, J.F. Bobo, D. Prost, F. Issac, F. Boust, J. Appl. Phys. 109 (2011) 07A323.
[11] M. Vroubel, Y. Zhuang, B. Rejaei, J. Burghartz, J. Magn. Magn. Mater. 258–259 (2003) 167.
[12] M. Ueno, S. Tanoue, J. Vac. Sci. Technol. A 13 (1995) 2194.
[13] Y. Liu, L.F. Chen, C.Y. Tan, H.J. Liu, C.K. Ong, Rev. Sci. Instrum. 76 (2005) 063911.
[14] F. Zhang, Y. Kitamoto, M. Abe, M. Naoe, J. Appl. Phys. 87 (2000) 6881.
[15] F. Xu, Q. Xie, N.N. Phuoc, S. Li, C.K. Ong, Thin Solids Films 519 (2011) 8292.
[16] G. Hinds, J.M.D. Coey, M.E.G. Lyons, Electrochem. Commun. 3 (2001) 215.
[17] S. Li, Z. Huang, J-.G. Duh, M. Yamaguchi, Appl. Phys. Lett. 92 (2008) 092501.
[18] N.N. Phuoc, L.T. Hung, C.K. Ong, J. Alloys Compd. 509 (2011) 4010.
[19] P. Zou, W. Yu, J.A. Bain, IEEE Trans. Magn. 38 (2002) 3501.
[20] T.L. Gilbert, IEEE Trans. Magn. 40 (2004) 3443.
[21] B.K. Kunar, R.E. Camley, Z. Celinski, J. Appl. Phys. 93 (2003) 7723.
[22] D. Spenato, S.P. Pogssian, D.T. Dekadjevi, J.B. Youssef, J. Phys. D: Appl. Phys. 40 (2007) 3306.
[23] S. Ge, S. Yao, M. Yamaguchi, X. Yang, H. Zuo, T. Ishii, D. Zhou, F. Li, J. Phys. D: Appl. Phys. 40 (2007) 3660.
[24] N.N. Phuoc, F. Xu, C.K. Ong, J. Appl. Phys. 105 (2009) 113926.
[25] A. Neudert, J. McCord, R. Schafer, L. Schultz, J. Appl. Phys. 95 (2004) 6595.
[26] H. Hoffman, IEEE Trans. Magn. 4 (1968) 32.
[27] J. Rantachle, C.Jr. Alexander, J. Appl. Phys. 93 (2003) 6665.
[28] G. Suran, H. Ouahmane, I. Iglesias, M. Rivas, J. Corrales, M. Contreras, J. Appl. Phys. 76 (1994) 1749.
[29] F. Xu, X.Y. Zhang, Y.G. Ma, N.N. Phuoc, X. Chen, C.K. Ong, J. Phys. D: Appl. Phys. 42 (2009) 015002.
[30] I.S. Jeong, A.P. Valanju, R.M. Weiser, J.H. Herring, J. Appl. Phys. 64 (1998) 5679.
[31] C. Kittel, Phys. Rev. 71 (1947) 270.
[32] F. Xu, X. Chen, Y.G. Ma, N.N. Phuoc, X.Y. Zhang, C.K. Ong, J. Appl. Phys. 104 (2008) 083915.
[33] J. McCord, R. Mattheis, D. Elefant, Phys. Rev. B 70 (2004) 094420.